IL NUOVO CIMENTO **47 C** (2024) 77
DOI 10.1393/ncc/i2024-24077-0

COLLOQUIA: IFAE 2023

Measurement of $t\bar{t}$ and Z-boson cross sections and their ratio using pp collisions at $\sqrt{s} = 13.6$ TeV with the ATLAS detector(*)

G. GUERRIERI(1)(2)(**) on behalf of the ATLAS COLLABORATION

(1) *INFN Sezione di Trieste - Trieste, Italy*
(2) *Università degli Studi di Udine - Udine, Italy*

received 13 February 2024

Summary. — The inclusive top-quark-pair production cross-section $\sigma_{t\bar{t}}$, the fiducial Z-boson production cross-section $\sigma^{\text{fid.}}_{Z\to\ell\ell}$, and their ratio are measured in the dilepton channel by the ATLAS collaboration using proton–proton collisions at the centre-of-mass energy of 13.6 TeV, employing 11.3 fb^{-1} of data collected in 2022 at the Large Hadron Collider. The top-quark-pair production cross-section is measured using events with an opposite-charge electron-muon pair and b-tagged jets, and corresponds to $\sigma_{t\bar{t}} = 859 \pm 4(\text{stat.}) \pm 22(\text{syst.}) \pm 19(\text{lumi.})$ pb. The Z-boson production cross-section is measured using e^+e^- and $\mu^+\mu^-$ final states in a fiducial phase space: $\sigma^{\text{fid.}}_{Z\to\ell\ell} = 751 \pm 0.3(\text{stat.}) \pm 15(\text{syst.}) \pm 17(\text{lumi.})$ pb. Finally, the ratio of the $t\bar{t}$ and the Z-boson production cross-sections is measured, benefiting from cancellation of several systematic uncertainties. The result for the ratio, $R_{t\bar{t}/Z} = 1.144 \pm 0.006(\text{stat.}) \pm 0.022(\text{syst.}) \pm 0.003(\text{lumi.})$ is consistent with the Standard Model prediction using the PDF4LHC21 PDF set.

1. – Introduction

The top quark is the heaviest known elementary particle; it was discovered in 1995 by the CDF [1] and D0 [2] experiments, and its large mass, close to the scale of electroweak symmetry breaking, gives it a unique role in the Standard Model (SM) of particle physics. The study of top quark–antiquark ($t\bar{t}$) production is an important part of the physics programme of the ATLAS [3,4] experiment at the CERN Large Hadron Collider (LHC) [5]. It allows quantum chromodynamics (QCD) to be probed at some of the highest reachable energy scales, and constitutes a crucial background in many searches for physics beyond the Standard Model (BSM). Therefore, precise measurements of the $t\bar{t}$ process are essential to fully exploit the discovery potential of the LHC.

(*) IFAE 2023 - "Energy Frontier" session
(**) E-mail: giovanni.guerrieri@cern.ch

2. – Analysis strategy

The aim [6] is two-fold. The first goal of the analysis is to provide an extensive validation and cross-checks of the new detector components, reconstruction and software used in the Run 3 of the LHC. The second, and the main goal, is to measure the inclusive $t\bar{t}$ cross-section in the dilepton final state. Furthermore, a cross-section ratio of $t\bar{t}$ over Z-boson is provided, with the aim to reduce experimental uncertainties, mainly the luminosity one. The analysis uses proton-proton collision data delivered by the LHC at CERN at a centre-of-mass energy of 13.6 TeV, and recorded by the ATLAS detector, representing an integrated luminosity of 11.3 fb^{-1}. Events with an opposite-charge dilepton pair, jets and b-tagged jets are considered.

The analysis exploits the so-called "b-tag counting" [7] technique, that simultaneously measures the $t\bar{t}$ cross-section and the b-jet identification efficiency in the $e\mu$ decay channel. This method has been shown to be effective in measuring the cross-section of the $t\bar{t}$ process in the dilepton decay channel due to its low sensitivity to systematic uncertainties. The strategy consists in selecting events with opposite-sign $e\mu$ pairs and counting the number of events that have one b-tagged jet (N_1) and two b-tagged jets (N_2), as described in the following:

$$N_1 = L\sigma_{t\bar{t}}\epsilon_{e\mu}2\epsilon_b\left(1 - C_b\epsilon_b\right) + N_1^{\text{bkg}}, \tag{1}$$

$$N_2 = L\sigma_{t\bar{t}}\epsilon_{e\mu}C_b\epsilon_b^2 + N_2^{\text{bkg}}, \tag{2}$$

where L is the integrated luminosity, $\sigma_{t\bar{t}}$ is the sought after cross-section of the $t\bar{t}$ production, ϵ_b is the efficiency to b-tag the jet after the selection, $\epsilon_{e\mu}$ is the efficiency for a $t\bar{t}$ event to pass the opposite sign $e\mu$ selection, C_b is a tagging correlation coefficient that is close to unity and $N_{1(2)}^{\text{bkg}}$ is the number of background events with one (two) b-tagged jets. The correlation factor, C_b, is defined as $C_b = \epsilon_{bb}/\epsilon_b^2$, where ϵ_{bb} represents the probability to reconstruct and tag both b-jets.

In this analysis, the technique described above is modified to be suitable for a binned profile-likelihood approach, in order to extract the $t\bar{t}$ production cross-section, the Z-boson production cross-section and the ratio of the cross-sections, $R_{t\bar{t}/Z}$. The Z-boson production cross-section $\sigma^{\text{fid.}}_{Z\to\ell\ell}$ is measured with events satisfying $66 < m_{\ell\ell} < 116$ GeV on the detector-level, matching the fiducial-phase-space definition.

3. – Objects definition and event selection

Electron candidates are reconstructed from electromagnetic clusters in the calorimeter matched to particle tracks inside the inner detector (ID). The candidates need to pass the *Tight* likelihood-based identification criteria [8] with $p_{\text{T}} > 27$ GeV and $|\eta| < 2.47$, with the transition region at $1.37 < |\eta| < 1.52$ excluded. Additionally, electron candidates need to fulfill impact parameter selection criteria: $|z_0 \sin\theta| < 0.5$ mm and $|d_0/\sigma(d_0)| < 5$.

Muon candidates are reconstructed from tracks from the muon spectrometer (MS) matched to tracks from ID. The candidates are required to pass *Medium* identification criteria [9] with $p_{\text{T}} > 27$ GeV and $|\eta| < 2.5$. Additionally, muon candidates need to pass $|z_0 \sin\theta| < 0.5$ mm and $|d_0/\sigma(d_0)| < 3$ selection.

To suppress non-prompt electrons or muons, charged leptons undergo additional isolation criteria based on the energy (momentum) deposited in the calorimeter (ID).

Jet candidates are reconstructed from clusters of topologically connected calorimeter cells using the *anti-k_t* [10] jet algorithm, and then calibrated using the *Particle flow* (PFlow) algorithm [11] that exploits both the calorimeter as well as ID information. After the calibration, jet candidates are required to have $p_{\mathrm{T}} > 30$ GeV and $|\eta| < 2.5$. To suppress pile-up jets, the neural network based NNJvt algorithm is used for jets with p_{T} below 60 GeV.

Jets containing b-hadrons are identified (b-tagged) using the DL1d [12] algorithm using the fixed 77% efficiency working point.

Events that pass at least one of the single-electron or single-muon triggers are selected. Moreover, events are required to have a reconstructed vertex with at least two tracks with $p_{\mathrm{T}} > 500$ MeV. Events are required to have exactly two leptons (electrons or muons) with opposite electric charge. In the same-flavour channels, events are required to have $66 < m_{\ell\ell} < 116$ GeV. The selection is inclusive in number of jets, even though in the $e\mu$ channel only events with one or two b-tagged jets are used in the analysis.

Figure 1 reports the leading lepton p_{T} distribution in data compared to the prediction for signal and background processes, as well as the distribution of the number of b-tagged jets used to extract the cross section values. Both distributions are presented for the $e\mu$ selection.

Moreover, from fig. 1 it is possible to appreciate the composition of the background, consisting of production of top quarks with W bosons (tW), Z+jets and diboson production, and fake and non-prompt leptons. The estimation of the latter is performed by checking the MC truth information to determine if the event that passed the selection contains a fake lepton or non-prompt lepton. Based on this truth information, the events are split into real and fake or non-prompt lepton contributions. Events classified as containing at least one fake or non-prompt lepton are combined into a single distribution, representing the estimate of the fake lepton contribution in data.

4. – Systematic uncertainties

The uncertainty in the integrated luminosity for data recorded in 2022 is 2.2%, whereas the uncertainty due to pile-up is determined by varying the average number of interactions per bunch-crossing by 4% in the simulation.

Lepton uncertainties are subdivided into two main categories: the first encompasses lepton momentum resolution and scales, while the second includes uncertainties originating from trigger, reconstruction, identification, and isolation efficiencies.

Jet Energy Scale (JES) and resolution (JER) uncertainties include the standard set of uncertainties estimated from Run 2. For the NNJvt discriminant, a conservative 10% uncertainty per b-tagged jet is applied.

For the efficiency of tagging a true b-jet, the uncertainties from the calibration using the Run 3 $t\bar{t}$ dilepton data is used. Uncertainties of 20% and 40% are applied respectively to mis-tag rates of c- and light-flavour jets.

Uncertainties due to the modelling of the $t\bar{t}$ signal include the parton shower and hadronisation model, variation of the renormalisation and factorisation scales in the matrix element (ME) by factors of 0.5 and 2, the variation of the Var3c parameter of the A14 tune [13], the choice of the h_{damp} parameter, and the top quark p_{T} distribution mismodelling.

Similarly to the $t\bar{t}$ uncertainties, scale variations in the ME, Var3c and for the final state radiation of the parton shower are considered for the tW process, together with an uncertainty due to the interference with the $t\bar{t}$ process.

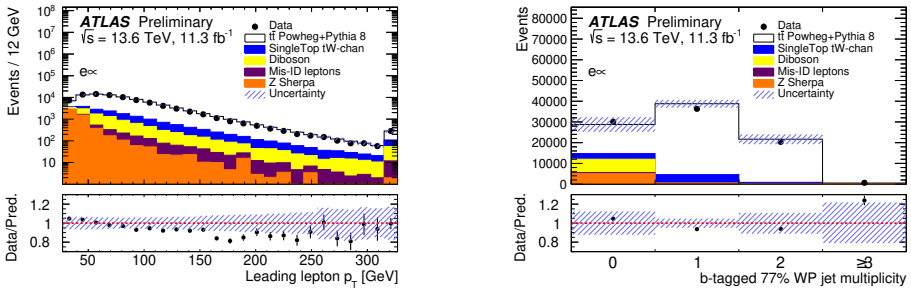

(a) (b)

Fig. 1.: Comparison of observed data and predictions for the (a) p_{T} of the leading lepton in $e\mu$ channel with an inclusive selection in number of jets, and the (b) distribution of the number of b-tagged jets in the $e\mu$ channel. The expected yields are calculated by normalising the MC prediction using the cross-section for each process and the estimate of the data integrated luminosity. The "Mis-ID" label represents fake and non-prompt leptons. The hashed band represents the total uncertainty. The bottom panel shows the ratio of data to prediction. The rightmost bins contain the overflow events. Figures taken from [6].

For the Z-boson sample, independent variations of the factorisation and renormalisation scales in the ME and the simultaneous variation of the parton shower by a factor of 0.5 and 2 are considered.

The PDF uncertainty is estimated by considering the internal variations of the PDF4LHC21 PDF set [14] for the $t\bar{t}$ and Z-boson samples.

A conservative normalisation uncertainty of 50%(100%) is assigned for the fake lepton background in the $e\mu$ channel with one(two) b-tagged jet(s). Additionally, a decorrelated, 100% uncertainty is assigned to the fake lepton estimate in the ee and $\mu\mu$ channels. A 50% uncertainty is considered for the normalisation of the diboson processes.

5. – Results

Figure 2 shows the distributions used in the fit to extract the $t\bar{t}$ cross-section, Z-boson production cross-section and the ratio of the cross-sections. The results of the fit are:

$$\begin{aligned}\sigma_{t\bar{t}} &= 859 \pm 4(\text{stat.}) \pm 22(\text{syst.}) \pm 19(\text{lumi.})\text{pb},\\ \sigma^{\text{fid.}}_{Z\to\ell\ell} &= 751 \pm 0.3(\text{stat.}) \pm 15(\text{syst.}) \pm 17(\text{lumi.})\text{pb},\\ \epsilon_b &= 0.548 \pm 0.002(\text{stat.}) \pm 0.004(\text{syst.}) \pm 0.001(\text{lumi.}).\end{aligned}$$

The ratio $R_{t\bar{t}/Z}$ is determined by repeating the fit replacing $\sigma_{t\bar{t}}$ by $R_{t\bar{t}/Z}$ as free parameter. This procedure takes into account all correlations among systematic uncertainties in the $t\bar{t}$ and Z-boson cross-section measurements. The obtained value is:

$$R_{t\bar{t}/Z} = 1.144 \pm 0.006(\text{stat.}) \pm 0.022(\text{syst.}) \pm 0.003(\text{lumi.}).$$

The predicted values for the cross-sections and the ratio for the fiducial phase space of the Z-boson with $Z \to \ell\ell$, where $\ell = e, \mu$, assuming a top-quark mass of 172.5 GeV

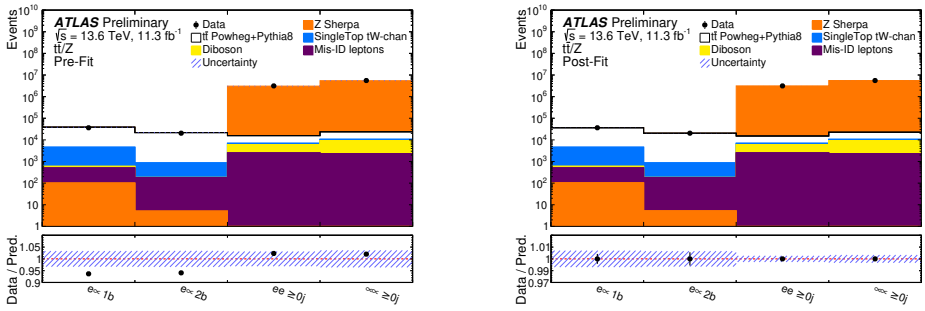

(a) (b)

Fig. 2.: Comparison of data and prediction for the event yields in the three lepton channels (a) before the fit, and (b) after the fit. The $e\mu$ channel is split into events with one or two b-tagged jets. The bottom panel shows the ratio of data over the prediction. The hashed bands represent the total uncertainty. Correlations of the NPs as obtained from the fit are used to build the uncertainty band in the post-fit distribution. Figures taken from [6].

and using the PDF4LHC21 PDF set are:

$$\begin{aligned} \sigma_{t\bar{t}}^{\text{theory}} &= 924^{+32}_{-40}(\text{scale} + \text{PDF})\ \text{pb}, \\ \sigma_{Z\to\ell\ell}^{\text{fid.,theory}} &= 741 \pm 15(\text{scale} + \text{PDF})\ \text{pb}, \\ R_{t\bar{t}/Z}^{\text{theory}} &= 1.245 \pm 0.076(\text{scale} + \text{PDF}). \end{aligned}$$

The ϵ_b value in the $t\bar{t}$ simulation is 0.545, compatible within the per mille uncertainty with the fitted value. The measurement of $\sigma_{t\bar{t}}$ is compatible at 1.3 standard deviations, when adding the prediction and measurement uncertainties in squares. The fitted Z-boson cross-section agrees with the prediction within one standard deviation. In fig. 3 the ratio of the $t\bar{t}$ and Z-boson production cross-sections is compared to the prediction for several PDF sets.

The largest source of systematic uncertainty in the individual cross-sections originates from the uncertainty in the luminosity estimation, followed by electron and muon reconstruction. For the cross-section ratio, the dominant uncertainty originates from the $t\bar{t}$ modelling, as it does not cancel out. Other significant uncertainties on the ratio include uncertainty in the trigger efficiencies and lepton reconstruction efficiencies.

6. – Conclusion

A measurement of the inclusive $t\bar{t}$ production cross-section, the fiducial Z boson production cross-section and the ratio of the cross-sections has been performed using 11.3 fb^{-1} of the LHC pp collision data collected by the ATLAS detector at a centre-of-mass energy of 13.6 TeV in 2022.

The $t\bar{t}$ cross-section is measured to be $\sigma_{t\bar{t}} = 859 \pm 4(\text{stat.}) \pm 22(\text{syst.}) \pm 19(\text{lumi.})$ pb. The measured value is compatible with the prediction at 1.3 standard deviations using the PDF4LHC21 PDF set and assuming top-quark mass of 172.5 GeV. The measured Z-boson cross-section is $\sigma_{Z\to\ell\ell}^{\text{fid.}} = 751 \pm 0.3(\text{stat.}) \pm 15(\text{syst.}) \pm 17(\text{lumi.})$ pb. The fitted value

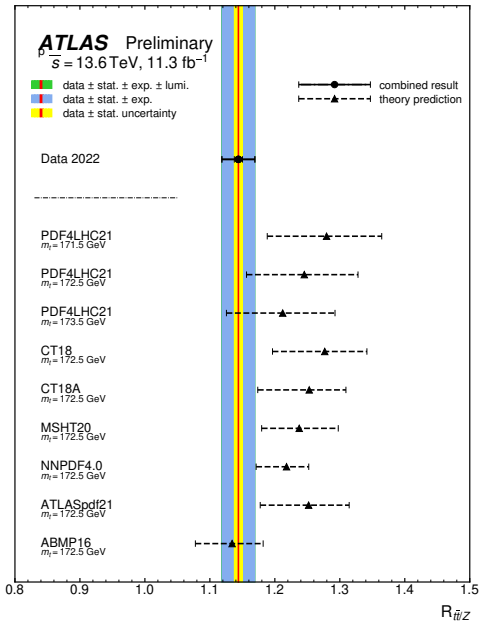

Fig. 3.: Ratio of the $t\bar{t}$ to the Z-boson cross-section compared to the prediction for several sets of parton distribution functions. For the PDF4LHC21 PDF set, predictions for different assumptions about the top-quark mass are also displayed. Figure taken from [6].

for the ratio is $R_{t\bar{t}/Z} = 1.114 \pm 0.006(\text{stat.}) \pm 0.022(\text{syst.}) \pm 0.003(\text{lumi.})$. The absolute cross-section measurements are limited by the uncertainty in the luminosity measurement as well as the lepton efficiency uncertainties, which cancel out to a large extent in the ratio measurement. The measured values are consistent with the SM prediction using the PDF4LHC21 PDF set.

REFERENCES

[1] CDF Collaboration, *Phys. Rev. Lett.*, **74** (1995) 2626.
[2] D0 Collaboration, *Phys. Rev. Lett.*, **74** (1995) 2422.
[3] ATLAS Collaboration, *JINST*, **3** (2008) S08003.
[4] ATLAS Collaboration, arXiv:2305.16623 (2023).
[5] Evans L. and Bryant P., *JINST*, **3** (2008) S08001.
[6] ATLAS Collaboration, ATLAS-CONF-2023-006 (2023).
[7] ATLAS Collaboration, *Eur. Phys. J. C*, **80** (2020) 528.
[8] ATLAS Collaboration, *Eur. Phys. J. C*, **79** (2019) 639.
[9] ATLAS Collaboration, *Eur. Phys. J. C*, **76** (2016) 292.
[10] Cacciari M. *et al.*, *JHEP*, **04** (2008) 063.
[11] ATLAS Collaboration, *Eur. Phys. J. C*, **77** (2017) 466.
[12] ATLAS Collaboration, ATL-PHYS-PUB-2022-047 (2022).
[13] ATLAS Collaboration, ATL-PHYS-PUB-2017-007 (2017).
[14] Ball R. D. *et al.*, *J. Phys. G*, **49** (2022) 080501.